



Enhanced red emission from $\text{CaZrO}_3:\text{Eu}^{3+}$ nano-phosphors prepared by Sol-gel technique

Subhash Chand*, Ishwar Singh and Devender Singh

M.D.U., Rohatk-124001, Haryana, India
drs Chopra78@gmail.com

Available online at: www.isca.in, www.isca.me

Received 2nd March 2018, revised 28th November 2022, accepted 12th January 2023

Abstract

Alkali metal ions codoped $\text{CaZrO}_3:\text{Eu}^{3+}$ nanophosphors series prepared by sol gel technique were further reheated to 750 °C to improve crystallinity of the product. The crystal structure and surface morphology of materials were determined by X-ray diffraction (XRD) and scanning electron microscopy (SEM) technique. XRD results confirmed orthorhombic perovskites structures of $\text{CaZrO}_3:\text{Eu}^{3+}$. The surface morphologies of materials were consisting of small, coagulated, cubical particles with smooth and regular surfaces. The characteristic strong red emissions of Eu^{3+} ions in $\text{CaZrO}_3:\text{Eu}^{3+}$, M (M= Li^+ , Na^+ , K^+) mainly at 613nm is due to $^5D_0 \rightarrow ^7F_2$ transitions and other weaker emissions were also observed at 575, 592, 654, and 698-705 nm corresponding to $^5D_0 \rightarrow ^7F_J$ (where J = 0, 1, 3, 4) transitions respectively. The remarkable increase of photoluminescence intensity corresponding to $^5D_0 \rightarrow ^7F_2$ transitions was observed in $\text{CaZrO}_3:\text{Eu}^{3+}$ if co-doped with Li^+ ions.

Keywords: $\text{CaZrO}_3:\text{Eu}^{3+}$, M (M= Li^+ , Na^+ , K^+); Orthorhombic; Sol gel; Photoluminescence.

Introduction

In the present time, researcher had major focus on the synthesis of trivalent rare earth ion doped perovskite-type phosphors due to their excellent luminescent property¹⁻³. Thus various kinds of ABO_3 type perovskites⁴⁻¹³ had been synthesized. As no major work for alkali metal ions codoped $\text{AZrO}:\text{Eu}^{3+}$ type perovskite phosphors prepared by sol gel synthesis have been reported till now. In these perovskites phosphor, Eu^{3+} ion act as a good activator¹⁴⁻¹⁶ for red emission due to the shielding effect of 5s and 5p electrons around the 4f shell of Eu^{3+} ion. Here, the series of $\text{CaZrO}_3:\text{Eu}^{3+}$, M (M= Li^+ , Na^+ , K^+) phosphors is prepared by sol gel method. The substitution of trivalent dopant by monovalent or divalent metallic ion leads to the formation of intrinsic defects which affect the luminescence intensity of phosphor. Hence to enhance the luminescence intensity, some alkali metal ions co-doping is done for compensating charge in the host lattice. I was guided to synthesize and characterize $\text{CaZrO}_3:\text{Eu}^{3+}$ by sol gel technique as this technique had already been used by us for preparing phosphor materials, because of its various attractive advantages^{17,18} such as simple experimental set-up, easy gel preparation and less time consuming as compared to traditional solid state method¹⁹. The gel combustion reaction occurring inside muffle furnace involves reaction between required metals and citric acid releases various gases and heat within a very short time, resulting product is fluffy, crispy and white crystalline powder containing nano-sized crystallites after sintering at 750°C had been prepared and characterized. The effect of co-doping of monovalent alkali ions (Li^+ , Na^+ , K^+) into $\text{CaZrO}_3:\text{Eu}^{3+}$ to enhance the photoluminescence intensity had been discussed and the possible mechanism has been proposed.

Material and Methods

Synthesis of Nano-phosphors: High purity (99.9%) chemicals like $\text{Ca}(\text{NO}_3)_2$, $\text{Zr}(\text{NO}_3)_4$ [1mol], $\text{Eu}(\text{NO}_3)_3$, NaNO_3 , KNO_3 , LiNO_3 , and Citric acid ($\text{C}_6\text{H}_8\text{O}_7$) from Aldrich were used to prepare a series of nano-materials having general formula $\text{Ca}_{(1-x)}\text{ZrO}_3:\text{Eu}^{3+}$ and $\text{Ca}_{(1-x+y)}\text{ZrO}_3:\text{Eu}^{3+}$, M [M= Li^+ , Na^+ , K^+] where x is 5 mol% and y is 1 mol% were prepared by heating slowly an aqueous concentrated mixture containing a calculated amount of metal nitrates and citric acid on a magnetic stirrer maintained at 150°C. The mixture undergoes slow dehydration and resulting viscous gel calcined inside muffle furnace maintained at 750°C for 3h to increase the crystallinity of the product.

Characterization of nanophosphor: The crystal structure characterization was performed by high resolution X-ray diffraction (XRD) using Rigaku Ultima IV diffractometer in the θ - 2θ configuration and using Cu $K\alpha$ radiation (0.154184 nm). The surface morphology of the phosphors was studied by using scanning electron microscope. Photoluminescence (PL) were examined using a He-Cd laser (325nm). Color purity was determined by using CIE 1931 chromaticity coordinates. All measurements were carried out at room temperature.

Results and discussion

Crystal structure determination: XRD spectra of the $\text{CaZrO}_3:\text{Eu}^{3+}$, M (M = Li^+ , Na^+ , K^+) phosphors are shown in Figure-1(a, b) indicate the presence of two extra phase like ZrO_2 [JCPDS No. 17-0923] and Eu_2O_3 [JCPDS Card No. 34-0392] and one main orthorhombic phase CaZrO_3 [JCPDS No. 35-0790] which accommodate the Eu^{3+} ions at Ca^{2+} site of matrix.

Some alkali ions like Li^+ , Na^+ and K^+ were co-doped in CaZrO_3 lattice successfully yet Li^+ and K^+ have large difference in ionic radii from that of Ca^{2+} . The ionic radii of Li^+ , Na^+ and K^+ is 76nm, 102nm, and 138 nm respectively, due to this difference of ionic radii of co-doped ions, the CaZrO_3 lattices have slight deformations leading to the variation in the heights of diffraction peaks. Thus effect of co-doping of alkali ions on $\text{CaZrO}_3:\text{Eu}^{3+}$ lattices had also been investigated to study the enhanced photo-luminescent intensity of the lattices.

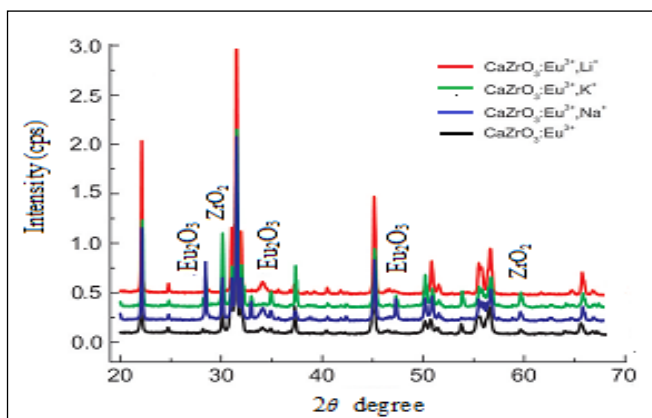


Figure-1(a): XRD spectra of $\text{CaZrO}_3:\text{Eu}^{3+}$ [Li^+ , Na^+ , K^+].

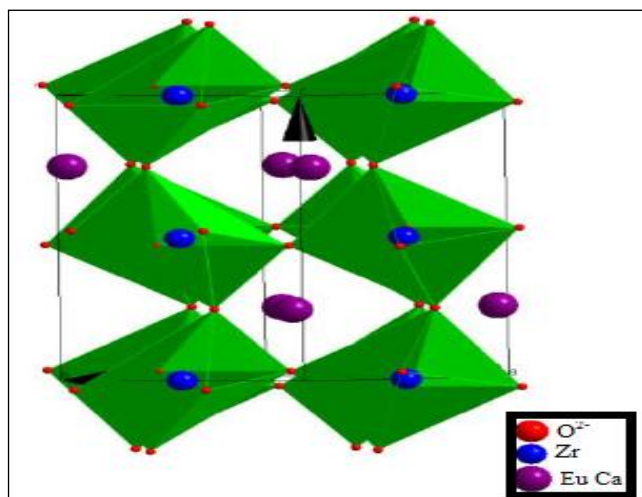


Figure-1(b): Orthorhombic phase structure of $\text{CaZrO}_3:\text{Eu}^{3+}$.

Because of smaller ionic size of Li^+ , there is a possibility of some of the Li^+ ions to reside in the interstitial sites between or among the host ions. This observation can be assigned due to the enormous changes in lattice constants of these samples. The unit cell constants and unit cell volumes of $\text{CaZrO}_3:\text{Eu}^{3+}$ samples as well as co-doped samples are calculated from the distance between the adjacent (200), (121), and (002) planes corresponding to diffraction peaks in Table-1.

Mari et al and coworker²⁰ observed that cell volume of the host compound increased if the larger ion like Eu^{3+} replace Ca^{2+} , Sr^{2+} cations in the host lattice,. Therefore, as shown in Table-1, the

cell volumes of $\text{CaZrO}_3:\text{Eu}^{3+}$, Na^+ and $\text{CaZrO}_3:\text{Eu}^{3+}$, K^+ after doping with Na^+ and K^+ ions increase, but decrease with the doping of Li^+ due to its smaller size. The cell volumes of $\text{CaZrO}_3:\text{Eu}^{3+}$, co-doped with mono-valent ions also follow the sequence, $\text{CaZrO}_3:\text{Eu}^{3+}$, K^+ > $\text{CaZrO}_3:\text{Eu}^{3+}$, Na^+ > $\text{CaZrO}_3:\text{Eu}^{3+}$, Li^+ ; having the increase in size of co-doped ions. The substitution of Li^+ at Zr^{4+} site causes more point defects in crystal lattice hence decrease the emission intensity of $\text{CaZrO}_3:\text{Eu}^{3+}$ materials. But the substitution of Li^+ at Ca^{2+} sites or at interstitial positions is more favorable and thus photoluminescence intensity also enhanced much more with the co-doping of Li^+ ion in $\text{CaZrO}_3:\text{Eu}^{3+}$.

Table-1: Calculated lattice parameters of $\text{CaZrO}_3:\text{Eu}^{3+}$ co-doped with Li^+ , Na^+ , K^+ .

Phosphor	a/nm	b/nm	c/nm	v/nm	Crystallite size
$\text{CaZrO}_3:\text{Eu}^{3+}$	0.57579	0.80181	0.55911	0.25808	20nm
$\text{CaZrO}_3:\text{Eu}^{3+},\text{Li}^+$	0.57519	0.80111	0.55679	0.25738	10nm
$\text{CaZrO}_3:\text{Eu}^{3+},\text{Na}^+$	0.57571	0.80241	0.55959	0.25850	20nm
$\text{CaZrO}_3:\text{Eu}^{3+},\text{K}^+$	0.57739	0.80389	0.56049	0.26015	20nm

SEM micrograph and particle size analysis: In Figure-2 (a, b) show the SEM micrograph of $\text{CaZrO}_3:\text{Eu}^{3+}$ and $\text{CaZrO}_3:\text{Eu}^{3+}$ co-doped with Li^+ ions containing smooth uniformity with agglomerated particles nearly cubical shape. The average size of particles in their SEM images lies between 10nm to 20nm.

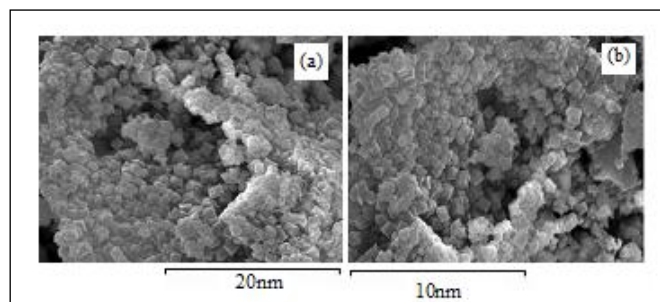


Figure-2: SEM micrograph of (a) $\text{CaZrO}_3:\text{Eu}^{3+}$, (b) $\text{CaZrO}_3:\text{Eu}^{3+},\text{Li}^+$.

Photoluminescence analysis :Figure-3 show room temperature emission spectra of $\text{CaZrO}_3:\text{Eu}^{3+}[\text{Li}^+, \text{Na}^+, \text{K}^+]$ were obtained using ultraviolet light at 325nm and emitted the red luminescence of varying intensities showed that the activator Eu^{3+} had successfully entered the host lattice of CaZrO_3 . These luminescence spectra of Eu^{3+} peak at 575nm, 592nm, 613nm, 654nm, and 698-705nm corresponding to $^5D_0 \rightarrow ^7F_0$, $^5D_0 \rightarrow ^7F_1$, $^5D_0 \rightarrow ^7F_2$, $^5D_0 \rightarrow ^7F_3$, and $^5D_0 \rightarrow ^7F_4$ transitions²¹⁻²⁴ respectively. The exact positions of emission peaks in various lattices are shown in Table-2.

Table-2: Position of various emission peaks (nm), India.

Phosphors	${}^5D_0 \rightarrow {}^7F_0$	${}^5D_0 \rightarrow {}^7F_1$	${}^5D_0 \rightarrow {}^7F_2$	${}^5D_0 \rightarrow {}^7F_3$	${}^5D_0 \rightarrow {}^7F_4$	$I_{(5D_0 \rightarrow 7F_2)} / I_{(5D_0 \rightarrow 7F_1)}$
CaZrO ₃ :Eu ³⁺	575	592	613	654	698 - 705	4.92
CaZrO ₃ :Eu ³⁺ ,Li ⁺	575	592	613	654	698 - 705	4.85
CaZrO ₃ :Eu ³⁺ ,Na ⁺	575	592	613	654	698 - 705	4.98
CaZrO ₃ :Eu ³⁺ ,K ⁺	575	592	613	654	698 - 705	4.85

It is well known that luminescence peaks of Eu³⁺ are sensitive to the symmetry around Eu³⁺ ions. The transition ${}^5D_0 \rightarrow {}^7F_2$ have dipole electric allowed one as well as dipole magnetic allowed when Eu³⁺ locates at a site of non-inversion symmetry, while ${}^5D_0 \rightarrow {}^7F_1$ magnetic dipole transitions only, at a site of inversion symmetry²⁵.

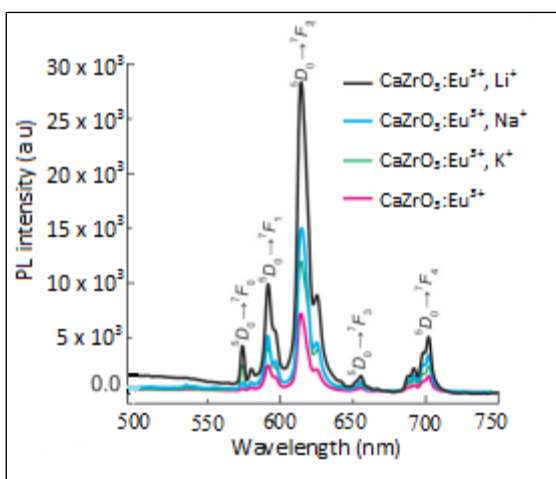


Figure-3: Photoluminescence spectra of CaZrO₃:Eu³⁺ co-doped with Li⁺, Na⁺, K⁺.

Usually the luminescence intensity ratio of ${}^5D_0 \rightarrow {}^7F_2$ to ${}^5D_0 \rightarrow {}^7F_1$ is regarded as a probe to detect the inversion environmental symmetry around Eu³⁺ in the host²⁶. On the basis of emission spectra shown in Figure-3, the ratio of transition ${}^5D_0 \rightarrow {}^7F_2$ to ${}^5D_0 \rightarrow {}^7F_1$ for CaZrO₃:Eu³⁺ samples and co-doped samples were calculated shown in Table-2. The intensity (I) ratio values for the transition $I({}^5D_0 \rightarrow {}^7F_2) / I({}^5D_0 \rightarrow {}^7F_1)$ are nearly 5 and 1 for CaZrO₃:Eu³⁺. Hence the photoluminescent intensity of CaZrO₃:Eu³⁺ is stronger confirming it a more suitable luminescent center for Eu³⁺ ions and a strong promising candidate for red display applications. The peak intensity is maximum in Li⁺ co-doped sample and minimum for K⁺ doped ions.

These emission lines were assigned to the *f-f* transitions of ${}^5D_3 \rightarrow {}^7F_4$, ${}^5D_2 \rightarrow {}^7F_j$ ($J=1, 2, 3$), ${}^5D_1 \rightarrow {}^7F_j$ ($J=1,2$). Hence the co-doping of Li⁺, Na⁺, K⁺ ion in CaZrO₃:Eu³⁺ phosphor increases the photoluminescence intensity in the following order: Li⁺ > Na⁺ > K⁺. The Li⁺, Na⁺, K⁺ ion decrease the intrinsic defects and

increases the energy transfer from host to charge transfer states as already observed by Mari et al, Co-worker and many other researchers²⁷⁻³¹ that the incorporation of mono-valent ions in CaTiO₃:Pr³⁺ creates oxygen vacancies, which might act as a sensitizer^{32,33} for effective energy transfer due to strong mixing of charge transfer states. Co-doping of mono-valent ions (mainly Li⁺ ion) increases energy transfer from Ca²⁺ to Eu³⁺ by reducing the surface defects. Here due to its small size, Li⁺ ion is substituted in the interstitial sites and increases the energy transfer from CaZrO₃ lattice to Eu³⁺ site.

Color purity analysis: Color chromaticity coordinates of CaZrO₃:Eu³⁺, Li⁺ are shown in Figure-4, calculated by the CIE 1931 color matching functions. The calculated value for CIE coordinates for CaZrO₃:Eu³⁺, Li⁺ are found to be $x=0.672$ and $y=0.329$, similar to the standard red color (0.670, 0.330) as observed in the National Television Standard Committee (NTSC) system.

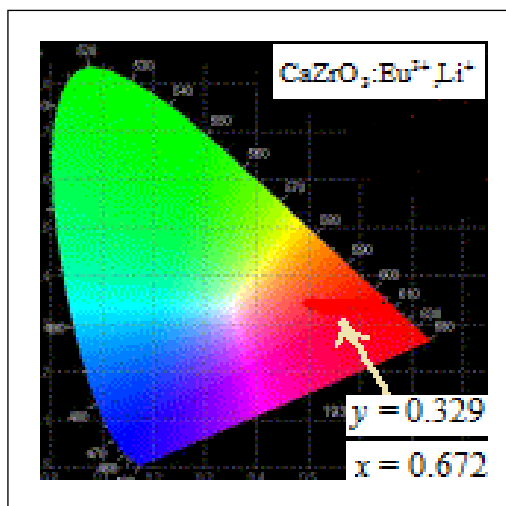


Figure-4: Color chromaticity diagram of CaZrO₃:Eu³⁺, Li⁺.

Conclusion

The X-ray diffraction study of CaZrO₃:Eu³⁺, M (M = Li⁺, Na⁺, K⁺) nano-materials prepared by sol gel technique confirm orthorhombic phase is the main phase in CaZrO₃:Eu³⁺ phosphor. The particle size of materials is in-between 10nm to 20nm. Hence on the basis of result obtained from characterization, it

can be concluded that Eu^{3+} and alkali metal ions substitute Ca^{2+} sites in CaZrO_3 lattices. This increase in the photoluminescence intensity of phosphor is due to increase of energy transfer from Ca^{2+} to Eu^{3+} ions mainly by co-doping of Li^+ ion. This remarkable increase in the photoluminescence intensity by co-doping with Li^+ ions in $\text{CaZrO}_3:\text{Eu}^{3+}$ lattices make them better candidates for various red luminescence display applications.

Acknowledgement

Author, Subhash Chand is heartedly thankful to thankful to Prof. K. C. Singh Ex. HOD, Department of Chemistry, M. D. University Rohtak, Haryana, India for timely providing the chemical assistance in the lab and also helped in the characterization of samples in IDF, Valencia-46022, Spain.

References

1. Huang J., Zhou L., Lan Y. and Gong, F. (2011). Synthesis and luminescence properties of the red phosphor $\text{CaZrO}_3:\text{Eu}^{3+}$ for white light-emitting diode application. *Central European Journal of Physics*, 9(4), 975-979. <http://dx.doi.org/10.2478/s11534-010-0132-7>
2. Chand S., Khatkar S.P. and Singh I. (2018). Improved energy transfer process in $\text{BaZrO}_3:\text{Eu}^{3+}$ nanophosphor synthesized by Sol-gel technique. *Res. J. Material Sci.*, 6(4), 1-6.
3. Singh D., Tanwar V. and Singh I. (2016). Rapid synthesis and enhancement in down conversion emission properties of $\text{BaAl}_2\text{O}_4:\text{Eu}^{2+},\text{RE}^{3+}$ ($\text{RE}^{3+}=\text{Y}, \text{Pr}$) nanophosphors. *J. Mater. Sci. Mater. Electron.*, 27(3), 2260-2266. <http://doi.org/10.1007/s10854-015-4020-1>
4. Boutinaud P., Pinel E., Dubois M., Vink A.P. and Mahiou R. (2005). UV-to-red relaxation pathways in $\text{CaTiO}_3:\text{Pr}^{3+}$. *J. Lumin.*, 111(1-2), 69-80. <https://doi.org/10.1016/j.jlumin.2004.06.006>
5. Okamoto S. and Amamoto H. (2001). Characteristic enhancement of emission from $\text{SrTiO}_3:\text{Pr}^{3+}$ by addition of Group-IIIb ions. *Appl. Phys. Lett.* 78(5), 655. <https://doi.org/10.1063/1.1343491>
6. Zhang H. X., Kam C.H., Zhou Y. and Chan Y.C. (2000). Green up conversion luminescence in $\text{Er}^{3+}:\text{BaTiO}_3$ films. *Appl. Phys. Lett.*, 77(5), 609. <https://doi.org/10.1063/1.127060>
7. García-Hernández, M., García-Murillo, A., de J. Carrillo-Romo, F., Jaramillo-Vigueras, D., Chadeyron, G., De la Rosa, E. and Boyer, D. (2009). Eu-doped BaTiO_3 powder and film from sol-gel process with polyvinylpyrrolidone additive. *International journal of molecular sciences*, 10(9), 4088-4101.
8. Zhang H., Li N., Li K. and Xue D. (2007). Structural stability and formability of ABO_3 -type perovskite compounds. *Acta Crystallographica Section B: Structural Science*, 63(6), 812-818. <https://doi.org/10.1107/s0108768107046174>
9. Singh V., Watanabe S., Gundu Roa T.K., Al-Shamery K., Haase M. and Dahl Jho Y. (2012). Synthesis, characterisation, luminescence and defect centres in solution combustion synthesised $\text{CaZrO}_3:\text{Tb}^{3+}$ phosphor. *J. luminescence*. 132(8), 2036-2042. <http://dx.doi.org/10.1016/j.jlumin.2012.03.027>
10. Zhang H.W., Fu X. Y., Niu S. Y. and Xin Q. (2008). Blue luminescence of nanocrystalline $\text{CaZrO}_3:\text{Tb}^{3+}$ phosphors synthesized by a modified Pechini Sol-gel method. *J. Lumin.* 128(8), 1348-1352. <http://dx.doi.org/10.1016%2Fj.jlumin.2008.01.007>
11. Huang J., Zhou L., Wang Z. and Lan Y. (2009). Photoluminescence Properties of $\text{SrZrO}_3:\text{Eu}^{3+}$ and $\text{BaZrO}_3:\text{Eu}^{3+}$ Phosphors with Perovskite Structure. *Journal of Alloys and Compounds*, 487(1-2), L5-L7. <http://dx.doi.org/10.1016/j.jallcom.2009.07.153>
12. Alarcon J, van der Voort D and Blasse G (1992). Efficient Eu^{3+} luminescence in non-lanthanide host lattices. *Mat Res Bull*, 27(4), 467-472. [https://doi.org/10.1016/0025-5408\(92\)90024-T](https://doi.org/10.1016/0025-5408(92)90024-T)
13. Mari B., C-Coca P., Singh K. C., Kaushik R. D. and OM Hari (2013). Preparation and Luminescence Properties of $\text{MZrO}_3:\text{Eu}^{3+}$, A ($\text{M}=\text{Ca}^{2+}, \text{Ba}^{2+}$; $\text{A}=\text{Li}^+, \text{Na}^+, \text{K}^+$) Phosphors with Perovskite Structure. *Acta Phys. -Chim. Sin.*, 29(6), 1357-1362. <https://doi.org/10.3866/PKU.WHXB201304032>
14. Joly A. G., Chen W., Zhang J. and Wang, S. (2007). Electronic energy relaxation and luminescence decay dynamics of Eu^{3+} in $\text{Zn}_2\text{SiO}_4:\text{Eu}^{3+}$ phosphors. *J. Lumin.*, 126(2), 491-496. <http://dx.doi.org/10.1016%2Fj.jlumin.2006.09.004>
15. Singh D. K., Baitha P. K. and Manam J. (2016). Enhancement of luminescence intensity and spectroscopic analysis of Eu^{3+} - activated and Li^+ charge-compensated CaTiO_3 color tunable phosphors for solid-state lighting. *Applied Physics A*, 122, 1-15. DOI <https://doi.org/10.1007/s00339-016-0201-x>
16. Xiao X. Yan B. (2007). Photoluminescence of $\text{Y}_{0.6}\text{Gd}_{0.4}\text{NbO}_4:\text{Eu}^{3+}/\text{Tb}^{3+}$ micrometric phosphors derived from hybrid precursors. *J. Mater. Lett.* 61(8-9), 1649-1653. <http://dx.doi.org/10.1016%2Fj.matlet.2006.07.092>
17. Lim H. S., Ahmad A. and Hamzah H. (2013). Synthesis of zirconium oxide nanoparticle by sol-gel technique. *AIP Conf. Proc.*, 31th Dec., 1571(1), 812. <https://doi.org/10.1063/1.4858755>
18. S. Ramesh, (2013). Sol-Gel Synthesis and Characterization of $\text{Ag}_{3(2+x)}\text{Al}_x\text{Ti}_{4-x}\text{O}_{11+\delta}$ ($0.0 \leq x \leq 1.0$) Nanoparticles. *J. Nanosci*, 1-9. <http://dx.doi.org/10.1155/2013/929321>
19. Izquierdo Pantoja M. T., Turan A., García S. and Maroto Valer M. (2018). Optimization of Li_4SiO_4 synthesis

- conditions by solid state method for maximum CO₂ capture at high temperature. 6, 3249-3257. <https://doi.org/10.1039/C7TA08738A>
20. Marí B., Moya M., Singh, I. and Chand S. (2012). Characterization and photoluminescence properties of some CaO, SrO and CaSrO₂ phosphors co-doped with Eu³⁺ and alkali metal ions. *Optical Materials*, 34(8), 1267-1271. <https://doi.org/10.1016/j.optmat.2012.01.032>
 21. Zhang H.W., Fu X. Y., Niu S. Y. and Xin Q. (2004). Low temperature synthesis of nanocrystalline YVO₄:Eu via polyacrylamide gel method. *J. Solid State Chem.*, 177(8), 2649-2654. <https://doi.org/10.1016/j.jssc.2004.04.037>
 22. Singh D. and Kadyan S. (2017). Synthesis and optical characterization of trivalent europium doped M₄Al₂O₉ (M = Y, Gd and La) nanomaterials for display applications. *J. Mat. Sci: Mat. in Elec.* DOI: <https://link.springer.com/article/10.1007/s10854-017-6901-y>
 23. Singh D., Tanwar V., Singh I. and Kadyan P.S. (2014). Synthesis and Luminescent Characterization of MAIO₃:Eu³⁺ Red Nanophosphors. *Adv. Sci. Lett.*, 20(7-9), 1726-1729. <https://doi.org/10.1166/asl.2014.5736>
 24. Singh D. and Tanwar V. (2017). Optical characteristics of Eu (III) doped MSiO₃ (M = Mg, Ca, Sr and Ba) Nanomaterials for white light emitting applications. *J. Mater. Sci. Mater. Electron*, 28(4), 3243-3253. <https://link.springer.com/article/10.1007/s10854-016-5914-2>
 25. Lin H., Liang H., Zhang G. and Su Q. (2011). The luminescence of Eu activated BaMg (BO) phosphors. *Applied Physics A: Materials Science & Processing*, 105(1), 143-147. <https://doi.org/10.1007/s00339-011-6465-2>
 26. Lu Z., Chen L., Tang Y. and Li Y. (2005). Preparation and luminescence properties of Eu³⁺-doped MSnO₃ (M = Ca, Sr and Ba) perovskite materials. *J. Alloy. Compd.*, 387 (1-2), L1-L4. <https://doi.org/10.1016/j.jallcom.2004.06.036>
 27. Blasse G. and Grabmaier B.C. (1994). How Does a Luminescent Material Absorb Its Excitation Energy? *Luminescent Materials*. Springer: Berlin, 10-32. ISBN: 978-3-642-79017-1
 28. Ryu H., Singh B. K., Bartwal K. S., Brik M. G. and Kityk, I. V. (2008). Novel efficient phosphors on the base of Mg and Zn co-doped SrTiO₃: Pr³⁺. *Acta Materialia*, 56(3), 358-363. <https://doi.org/10.1016/j.actamat.2007.09.041>
 29. Diallo P. T., Jeanlouis K., Boutinaud P., Mahiou R. and Cousseins J. C. (2001). Improvement of the optical performances of Pr³⁺ in CaTiO₃. *Journal of alloys and compounds*, 323, 218-222.
 30. Tang J., Yu X., Yang L., Zhou C. and Peng X. (2006). Preparation and Al³⁺ enhanced photoluminescence properties of CaTiO₃:Pr³⁺. *Mater. Lett.* 60(3), 326-329. <https://doi.org/10.1016/j.matlet.2005.08.047>
 31. Mari, B., Singh, I. Singh, K.C., Cembrero-Coca, P., Singh, D. and Chand, S. (2013). Red emitting MTiO₃ (M = Ca or Sr) phosphors doped with Eu³⁺ or Pr³⁺ with some cations as co-dopants. *Displays*, 34(4), 346-351. <http://dx.doi.org/10.1016/j.displa.2013.07.003>
 32. Yin Q., Qui K., Chen Y., Liu J. and Xiao X. (2020). Enhancements of luminescent properties of CaTiO₃: Dy³⁺, Pr³⁺ via doping M⁺ = (Li⁺, Na⁺, K⁺). *Materials Letters* 127488, 266(668). <https://doi.org/10.1016/j.matlet.2020.127488>
 33. Kumar M., Vijayalakshmi R.P. and Rtanakaram Y.C. (2022). Investigation of structural and optical properties of Pr³⁺ doped and Pr³⁺/Dy³⁺ co-doped multicomponent Bismuth phosphate glasses for visible light applications. *Journal of Molecular Structure*, 1265(3), 133333. <http://dx.doi.org/10.1016/j.molstruc.2022.133333>